Doklady Earth Sciences, Vol. 375, No. 8, 2000, pp. 1329–1334. Translated from Doklady Akademii Nauk, Vol. 375, No. 2, 2000, pp. 239–244.

GEOPHYSICS

Monitoring of Stressed State in the Aftershock Region of the Spitak Earthquake

Yu. L. Rebetskii, S. S. Aref'ev, and E. S. Nikitina

Presented by Academician V. N. Strakhov February 3, 2000

Received February 21, 2000

INTRODUCTION

The primary purpose of this work consists of the optimization of principles for spatiotemporal monitoring of the stressed state in a region with active seismicity. In the framework of the stated problem, regions of catastrophic earthquakes, for which aftershock source mechanisms were determined by the local network of teleseismic stations, seem most promising. The experimental basis for reconstructing the stressed state was composed of 298 source mechanisms of aftershocks (magnitudes $M_s \sim 1.5$–3.5) within the source zone of the Spitak earthquake during the period from December 25, 1988 to January 8, 1989. The aftershocks were recorded by the temporal system of observations during joint field work carried out by the Schmidt Joint Institute of Physics of the Earth (Russia) and the Institute of Physics of the Earth, Strasburg University (France) [9]. Their magnitudes lie chiefly within the range 1.5–3.5, and only the eighteen strongest aftershocks have magnitudes $3.5 < M_s < 4.8$. It should be also noted that seven hundred and eight earthquakes were recorded during the specified period in the region under investigation; however, the ones mentioned had a sufficient number of determinations of the first arrival signs for calculating their mechanisms to an acceptable accuracy.

The identification of five zones with different seismic regimes and associated tectonic fractures was one of the results of the previous investigations carried out in the aftershock region [10]. The activity of these fractures manifested itself both during the main shock and aftershock period. The tectonic scheme of the region with the epicenters of earthquake sources used for the reconstruction is presented in Fig. 1a. The mechanisms of earthquakes with the magnitude $M_s > 3.5$ (the data were collected and prepared by J.Ya. Aptekman) and their depth distribution in the projection onto the latitudinal and longitudinal cross sections are also shown here (Figs. 1b, 1c). Later investigations of the seismological data obtained in the epicentral region of the Spitak earthquake made it possible to perform deep tomography of this region [2]. According to its results, two deep layers with velocities of 5.3 and 6.0 m s^{-1}, interpreted as the sedimentary cover and consolidated basement, respectively, with the interface at a depth of about 4 km, were identified. It was suggested that several sites exist with anticlinical uplifts of the more rigid basement, with which the sources of relatively stronger aftershocks are associated [2]. The data on aftershock source mechanisms made it possible to arrive at the conclusion that the predominant type of displacement in the aftershock sources varies owing to mechanically different types of repeated shocks in the central part and margins of the source zone [1].

METHOD

The method of cataclastic analysis of sets of shear fissures or earthquake source mechanisms [6] is the main tool used in the present work for reconstructing the tensors of tectonic stresses and seismotectonic deformation increments. This method includes a group of physical criteria for the identification of spatiotemporal boundaries of macrovolumes with a homogeneous deformation. Therefore, we can apply this method for monitoring temporal changes in the stressed state of regions with high seismic activity.

The preliminary analysis of the initial seismological data showed that the predominant size of the regions with elastic release for separate earthquakes (~ 2–$3L_{source}$) in the considered range of magnitudes ($M_s = 1.5$–3.5) was much less than the seismically active layer (12 km), and the density of their distribution is sufficient for the statement of the problem about the reconstruction of deformation process parameters for different deep sections. It is the last circumstance that enabled the stressed state reconstruction in nodes of the three-dimensional grid with a step of 0.02° in the lateral direction and 2 km in depth.

The compilation of homogeneous aftershock samplings was preceded by the compilation of the initial sampling of earthquakes. In this case, the basic proce-

Schmidt Joint Institute of Physics of the Earth (OIFZ), Russian Academy of Sciences, Bol'shaya Gruzinskaya ul. 10, Moscow, 123810 Russia

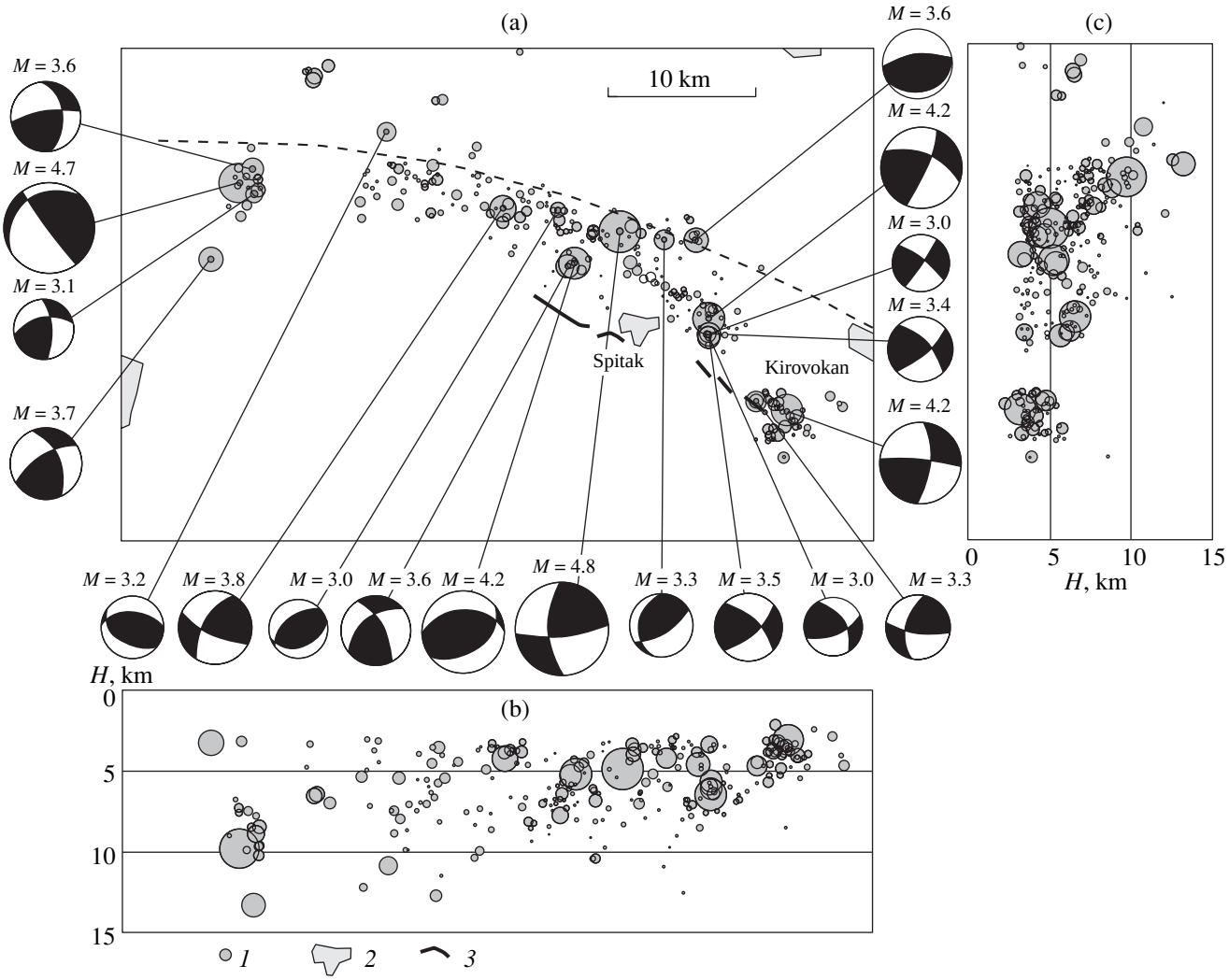

Fig. 1. (a) Tectonic scheme of the region with source epicenters of earthquakes of $M_S < 5$ and mechanisms of earthquakes with $M_S > 3$. The distribution of sources in cross sections in the (b) latitudinal and (c) longitudinal directions. (*1*) Earthquake sources; (*2*) populated areas; (*3*) fractures.

dure was to select earthquakes whose elastic release regions incorporate the point for calculating the parameter stress tensors and seismotectonic deformation increments (the grid node). After initial sampling of aftershocks based on this procedure, temporal scanning of the grid was accomplished in each node. This procedure was performed by successively selecting one of the aftershocks from the initial sampling as the first event of the homogeneous sampling. Furthermore, this sampling was increased owing to a successive incorporation of aftershocks located first in the negative direction (on the timescale) from the first event of the homogeneous sampling and then in the positive direction. In this case, principles of the positive and monotonic character of the dissipative process were verified [6]. The compilation of the homogeneous sampling terminated after two cases of incompatibility of the analyzed aftershock mechanisms with the specified principles or after the completion of the analysis of all events from the initial sampling.

CALCULATIONS

The reconstruction of the local field of stresses and seismotectonic deformations in the aftershock region of the Spitak earthquake was preceded by the reconstruction of parameters characterizing the tensors of tectonic stresses and seismotectonic deformation increments at the regional level. The data on source mechanisms of earthquakes with magnitudes $M_S > 5$ (altogether six events from 1976 to 1990) from the CMTS Catalog (Harvard University) [8] were used. The reconstruction yielded the parameters which determined the orientation of principal axes (strike azimuth and dip angle) and the ellipsoid type (the Lode–Nadai coefficient) for the tensors of stresses and seismotectonic deformation increments, respectively (table).

Table 1.

Tensor	Axis 1		Axis 2		Axis 3		Lode–Nadai coefficient
	azimuth	dip	azimuth	dip	azimuth	dip	
σ	270°	18°	56°	69°	176°	11°	0.5
$d\varepsilon$	264°	6°	13°	72°	174°	17°	0.5

The comparison of the parameters presented in the table indicates that the deviation of the calculated tensors from coaxiality lies within the accuracy of the calculation of the orientation of principal axes (15°, according to our data). Results of the reconstruction on two lower hemisphere diagrams are presented in Fig. 2. Here, areas with different shades characterize the degree of discrepancy between the compiled homogeneous sampling of earthquakes and the stress tensor when the relevant principal stress axis emerges at the given point of the sphere.

Results of the tensor parameter reconstruction of seismotectonic deformation increments are depicted in Fig. 3 for the depth levels of grid node location 2, 4, 6, 8, and 10 km for two time intervals identified by the reconstruction results (each figure represents the orientation of trajectories of the projections of maximum elongation and shortening axes from the top to bottom in order of increasing depth). The first time interval determined the stress field formed by January 1, 1989 mainly due to previous earthquakes, whereas the second time interval corresponded to the terminal stage of observations. The main contribution to the field formation during the second time interval was made by earthquakes after January 5, 1989. Figure 3 shows trajectories of axes with the maximum and minimum deviatoric shortening acting in the horizontal plane together with the orientation of the projections of axes with the principal shortening onto this plane (the arrows show the dip direction of these axes). It should be noted that the axes with the principal shortening are subhorizontal for the study region (the deviation of the specified axes from the horizontal plane does not exceed 15° in the central and eastern sectors of the aftershock region and 30° in the western sector). Apart from the reconstruction results, the source mechanisms of relatively strong aftershocks with magnitudes $M_s > 3$ are also presented in Fig. 3.

DISCUSSION

The analysis of the results allows us to infer that the field of seismotectonic deformations and the field of stresses for both of the temporal stages characterize the process of seismotectonic flow of rock masses associated with the activity of the following fractures: the deep-seated fracture between the Spitak and Gekhasar Settlement traced at the surface by the upthrust-type dislocations [7], the northwestern segment of the extended dextral Alavar fracture, the deep-seated fracture along the southern slope of the Bazum Ridge, and the upthrust-type segment of the Pambak–Sevan fracture. Based on results of stage 1 reconstruction (Fig. 3a), one should note the characteristic underturns of the axes with the maximum deviatory shortening towards the strike of the deep-seated Spitak–Gekhasar fractures, along the southern slope of the Bazum Ridge, and the eastern segment of the Pambak–Sevan fracture. Here, the angle between shortening axes and the fracture plane diminishes with depth from 45° to 30° (the Pambak-Sevan fracture), from 30° to 20° (the Bazum Ridge) and from 30° to 15° (Spitak–Gekhasar). It is important to note that a sharp change in the orientation of axial trajectories with the maximum shortening is observed directly within the Spitak region. Here, these

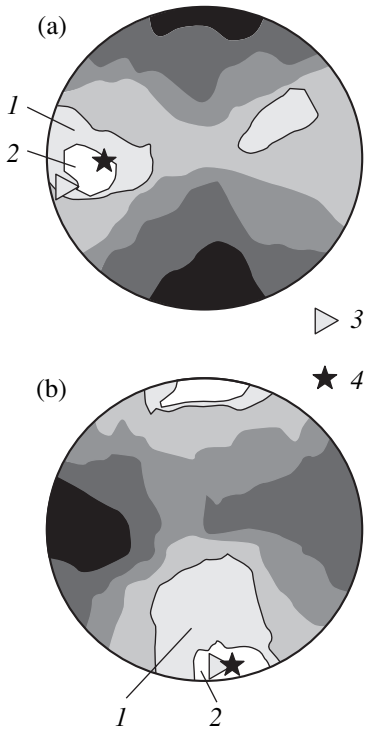

Fig. 2. Results of the reconstruction of the regional tensor of tectonic stresses and the tensor of seismotectonic deformation increments on the lower hemispheres: (a) σ_1, $d\varepsilon_1$ and (b) σ_3, $d\varepsilon_3$. (*1*) Regions with the permissible "exit" of principal axes of the tensor of seismotectonic deformation increments; (*2*) regions with the permissible "exit" of principal axes of the stress tensor; (*3*) principal axes of the tensor of seismotectonic deformation increments; (*4*) principal axes of the stress tensor.

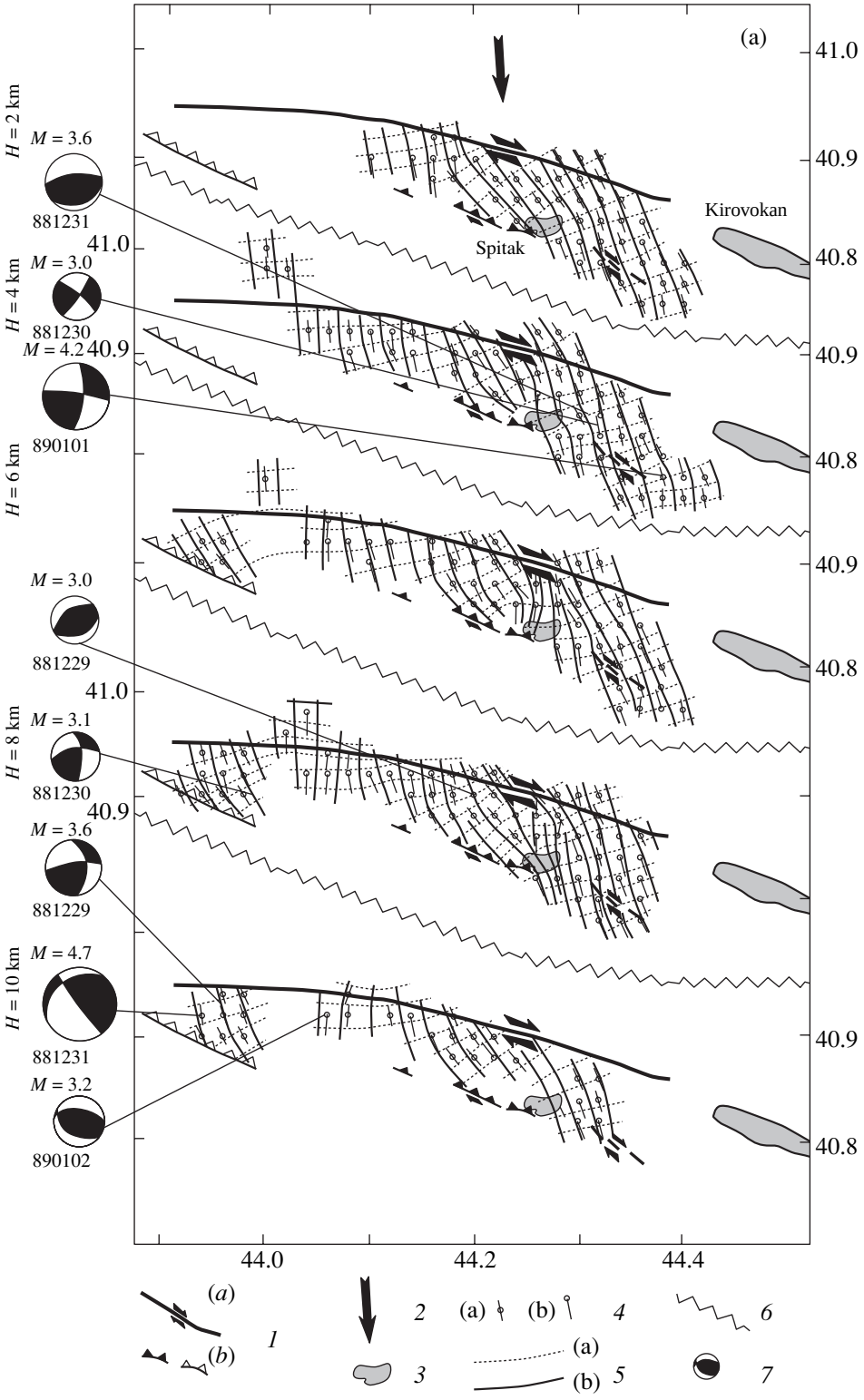

Fig. 3. Schematic parameters of the tensor of seismotectonic deformation increments at different depth sections for two time stages: (a) from December 25, 1988 to January 1, 1989, (b) from January 5, 1989 to January 9, 1989. (*1*) Fractures of (*a*) strike-slip and (*b*) upthrust types; (*2*) orientation of the axis with the maximum shortening of compression of the regional tensor of seismotectonic deformation increments (table); (*3*) populated areas; (*4*) principal axes of shortening of the local tensor of seismotectonic deformation increments with dip angle (*a*) < 6° and (*b*) > 6°; (*5*) trajectories with the (a) maximum and (b) minimum shortening in the horizontal plane of the local tensor of seismotectonic deformation increments; (*6*) source mechanisms of earthquakes with $3 < M_S < 5$; (*7*) edge lines of the maps with different depth levels.

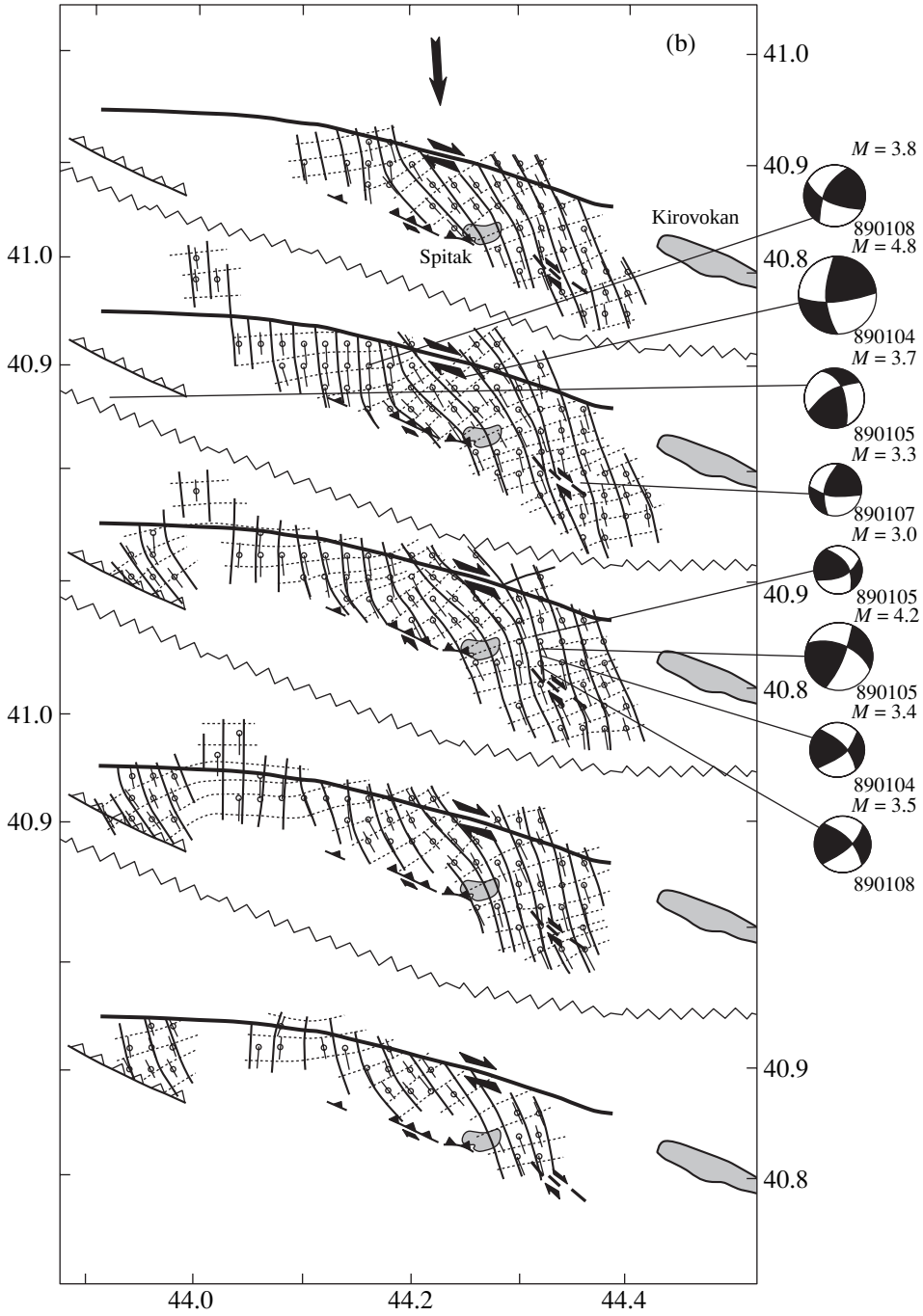

Fig. 3. (Contd.)

axes turn practically subnormal toward the deep-seated fracture strike. These regularities are most intensely manifested at a depth of 6 km, less intensely manifested at depths of 2, 4, and 8 km, and are practically absent in the lower layer (10 km). As is known [5], such a change in the orientation of trajectories of principal stress axes and deformation is typical for terminal regions of active fractures. It should be also noted that the displacement northward of the region with subnormal underturns of principal stresses toward the fracture strike with increasing of depth agrees with the northward dipping of the system of source planes of the Spitak earthquake.

The specified features of the seismotectonic deformation field suggest the absence of any unified seismotectonic flow along the Spitak–Gekhasar and Spitak–Alavar deep-seated fracture systems at the first stage. The existence at the first stage of two separate areas of active seismotectonic creep along the eastern and west-

ern source segments with the interface along the Aragats–Spitak lineament, which is incorporated into the lineament system of the Transcaucasian transverse uplift, can also probably explain the structure of the field of the reconstructed seismoactive deformation tensor. The separate seismotectonic flows along the Spitak–Gekhasar and the Spitak–Alavar fracture systems can be caused by both changes in the strike of deep-seated fractures and the existence of abyssal structural inhomogeneities. The structural inhomogeneity, revealed by an analysis of lineaments precisely for a depth of 7 km near the intersection of the Aragats–Spitak lineament with the Pambak–Sevan and Alavar fractures, was described in [4].

Results of the reconstruction of the tensor of seismotectonic deformation increments for the last time interval are presented in Fig. 3b. This interval is characterized by the formation of a unified region of seismotectonic flow along the whole system of the Spitak–Gekhasar and Spitak–Alavar deep-seated fractures. This process is governed by a sufficiently high smoothness of the trajectories of principal axes of the tensor of seismotectonic deformation increments at the intersection of these faults with the Aragats–Spitak lineament. Such a regular change in the orientation of these axes suggests that seismic activity at previous stages resulted in the destruction of bulkheads preventing the formation of a unified dextral fracture at depths of 4 to 8 km. The position of the three strongest aftershocks with magnitudes $M_s > 4.2$ from January 3, 1989 to March 5, 1989 precisely falls on the supposed detachment region (Fig. 3b).

CONCLUSIONS

The principles for creating homogeneous samplings of seismological data on earthquake source mechanisms and for finding spatiotemporal boundaries of macrovolumes with a uniform deformation have been elaborated on the basis of results of aftershock sequence processing. The investigations performed have made it possible to conclude that principles of the cataclastic analysis method can be used for identifying the phases of stable seismotectonic flow of rock massifs.

Results of the reconstruction of the stressed and strained state in the source zone of the Spitak catastrophic earthquake have made it possible to reveal the constrained deformation zone at depths of 4–8 km near Spitak for the initial stage of the processed aftershock sequence.

More detailed results regarding the reconstructed parameters of the tensors of tectonic stresses and seismotectonic deformation increments with the possible scanning of changes of the parameters of these tensors in the aftershock region of the Spitak earthquake in the monitoring regime will be presented on the website of the Laboratory of Tectonophysics, OIFZ, at the address: http://www.dino.scgs.ru/ipe1/tph/pub after the publication of this work.

ACKNOWLEDGMENTS

The authors are grateful to J.Ya. Aptekman for sharing her seismological data and participation in discussing the investigations performed.

This work was supported by the Russian Foundation for Basic Research, project nos. 98-05-64794 and 99-05-65417.

REFERENCES

1. Aptekman, Zh, Ya., Lander A.V., Dorbat K., and Dorbat L., *Izv. Akad. Nauk SSSR, Fiz. Zemli,* 1991, no. 11, pp. 96–105.
2. Dorbat, L., Aref'ev, S.S., and Borisov, B.A., *Fiz. Zemli,* 1994, no. 7/8, pp. 42–52.
3. Ivlev, D.D. and Bykovtsev, G.I., *Teoriya uprochnyayushchegosya plasticheskogo tela* (Theory of the Strengthening of a Plastic Body), Moscow: Nauka, 1971.
4. Nechaev, Yu.V. and Ragozhin, E.A., *Dokl. Akad. Nauk SSSR*, 1991, vol. 320, no. 6, pp. 1441–1445.
5. Osokina, D.N. and Fridman, V.N., *Polya napryazhenii i deformatsii v zemnoi kore* (Stress-and-Strain Fields in the Earth's Crust), Moscow: Nauka, 1987, pp. 74–119.
6. Rebetskii, Yu.L., *Dokl. Akad. Nauk*, 1999, vol. 365, no. 3, pp. 392–394.
7. Rogozhin, E.A. and Filip, E., *Fiz. Zemli*, 1991, no. 11, pp. 3–17.
8. Dziewonski, A.M., Chou, T.-A., and Woodhouse, J.H., *J. Geophys. Res.*, 1981, vol. 86, pp. 2825–2852.
9. Dorbath, L., Dorbath, C., Rivera, L., *et al.*, *Geophys. J. Int.*, 1992, vol. 108, pp. 309–328.
10. Haessler, H., Deshamps, A., Dufumier, H., *et al., Geophys. J.*, 1992, vol. 108, pp. 1–11.